JSR Publications

Available Online

J. Sci. Res. **17** (3), 879-899 (2025)

JOURNAL OF SCIENTIFIC RESEARCH

www.banglajol.info/index.php/JSR

Synthesis, Characterization and Electrochemical Studies of 2-Amino-4-Phenylthioazole based Azo Dyes

P. H. Kusuma[1], C. T. Keerthikumar[1*], C. T. Ramyakumari[2], T. M. Raghavendra[1]

[1]Department of Studies in Chemistry, Davangere University, Shivagangotri, Davangere-577007 Karnataka, India

[2]Department of Chemistry, D. R. M Science College, Davangere -577002, Karnataka, India

Received 19 December 2024, accepted in final revised form 28 May 2025

Abstract

The present work outlines the synthesis and characterization of heterocyclic azo dyes derived from 2-amino-4-phenylthiazole through the diazo coupling process. The coupling compounds were 4-hydroxycoumarin, 2,4-dihydroxybenzophenone, and 2-hydroxy-4-methoxy benzophenone. The synthesis was carried out under optimal experimental conditions at temperatures between 0 °C and 0.5 °C, reddish, reddish-orange, and reddish-yellow colors in good yields (50–75 %), they were characterized using various spectroscopic techniques like FT-IR all synthesized compounds exhibited characteristic azo group peaks in the range of 1400–1490 cm^{-1}. The UV-visible spectra were recorded in solvents such as DMSO, ethanol, and acetone. ^{1}H-NMR spectra OH groups in the compounds were observed at specific chemical shifts: A1 at 12.569 ppm, A2 at 12.223 and 10.850 ppm, and A3 at 12.092 ppm. The ^{13}C-NMR spectra to identify carbon environments and further validate the molecular structure. The mass spectra of the compounds showed [m+1] ionic peaks corresponding to their molecular weights confirming the formation of the azo dyes. The electrochemical behavior of the azo compounds was studied using a glassy carbon electrode (GCE) in a 0.1M H_2SO_4 solution. The study investigated the effect of scan rates (50–250 mV/s) and concentrations (10–50 µM) on the redox properties of the compounds. Irreversible process of the azo center underwent an irreversible reduction involving the consumption of four electrons.

Keywords: 2-Amino-4-phenylthiazole; Azo dyes; Cyclic voltammetry; Glassy carbon electrode.

doi: https://dx.doi.org/10.3329/jsr.v17i3.78549 J. Sci. Res. **17** (3), 879-899 (2025)

1. Introduction

Azo dyes are synthetic dyes characterized by the presence of one or more azo (-N=N-) groups [1]. They are widely used in food, cosmetics [2], and pharmaceuticals due to their vibrant colors and stability [3]. Azo dyes have been extensively studied for their applications in high-tech industries, particularly in fields like non-linear optical (NLO) materials, inkjet printing [4], photo-sensitizers [5], and textile coloring [6]. Their unique

*Corresponding author: drkeerthikumarct@gmail.com

electronic structures, stability, and tunable optical properties make them ideal candidates for these applications [7]. Azo dyes are among the most significant subcategories of synthetic dyes due to their simple synthesis [8], and broad color spectrum [9], enabling the production of dyes with various shades and properties [10]. Thiazole-based azo dyes have a strong affinity for synthetic and natural fibers, making them suitable for polyester [11], cotton, wool, and nylon [12]. Their ability to form strong interactions with fabric molecules leads to high color fastness and resistance to washing and fading [13]. These dyes exhibit bright shades ranging from yellow, orange, red, and violet to deep blue [14]. The thiazole ring improves the thermal and photochemical stability of azo dyes [15], ensuring long-lasting color retention [16,17]. Electrochemical techniques are widely used for molecular detection due to their simplicity, high sensitivity, and fast response times [18]. Specifically, these azo dyes have been investigated using cyclic voltammetry with a glassy carbon electrode, highlighting their redox behavior [19,20]. The presence of functional groups containing sulfur, nitrogen, and oxygen atoms in these dyes likely contributes to their adsorption affinity on metal surfaces [21,22].

Electrochemical behavior of azo-dyes, particularly focusing on how azo compounds undergo chemical reduction and produce hydrazo derivatives, which involves breaking the –N=N– bond to form primary amine molecules [23]. Electrochemical reduction is highlighted as a key method for investigating the mechanism and kinetics of these reactions [24]. The cyclic voltammetric technique was used to investigate the relationship between effect of scan rate and concentration [25,26]. Previously, we synthesized thiazole azo dyes and derivatives, azo dyes based on amino thiadizole; antipyrine, aniline and sulfamethazine moiety-based azo dyes to explore their application [27,28].

In this regard, the synthesis and electrochemical studies of heterocyclic azo dyes was the main topics of our present research work. Through a diazotization procedure, 2-amino-4-phenylthioazole was converted to its equivalent diazonium salt. It was then coupled with different coupling components at 0–5˚C and characterized using a different of spectroscopic and analytical methods. Further electrochemical investigation of these azo compounds was carried out and also studied at glassy carbon electrode by using cyclic voltammetric technique. The results showed that reduction of azo dye occurs through two irreversible reduction peaks and the reduction mechanism was proposed and discussed.

2. Materials and Methodology

2.1. *General*

Chemicals and solvents were purchased from (99% Sigma Aldrich, India). The cmhmicals uncorrected melting points were measured using an electrothermal instrument. Other chemicals were HCl, H_2SO_4 (98 %, Nice, India), $NaNO_2$, and KOH (S. D. Fine-Chem Limited, India), DMSO, ethanol, and acetone were purchased from (99 %, Spectrochem, India). The synthesized compounds were characterized by FT-IR spectra recorded using the ALPHA II Bruker IR spectrometer operating in the 400–4000 cm^{-1} range. The Shimadzu

UV-1900 Probe spectrophotometer was used to do electronic spectrum measurements in the 200–600 nm range. A JEOL 400 MHz and model JNM-ECZ400/L1 resolution multinuclear spectrometer were used to record ^{1}H NMR and ^{13}C NMR spectra at 300 K in tetramethylsilane (TMS) in the DMSO-d6 solution as an internal standard. A mass spectrometer (Xevo G2-XS QT) and CHI660E electrochemical workstation were used for the cyclic voltammetric studies.

2.2. *Azo dyes*

2-amino-4-phenylthiazole was diazotized in acidic medium, and then it was coupled with 4-hydroxycoumarine, 2.4-dihydroxybenzophenone, and 2-hydroxy-4-methoxybenzo phenone.

2.2.1. *Preparation of 2-amino-4-phenylethiaole azo dye (A1-A3)*

2-Amino-4-phenylthiazole (0.003 mol, 0.50 g) is dissolved in 4 mL of concentrated HCl. The solution is rapidly chilled in a salt/ice bath to 0–5 °C. A solution of sodium nitrate (0.003 mol, 0.26 g) is mixed with 3 mL of concentrated sulfuric acid (at 50 °C) to prepare nitrosyl sulfuric acid. The amine solution is cooled for half an hour before this reagent is added. The diazonium salt is allowed to develop by stirring the mixture for two hours more at 0 °C. An aqueous KOH solution containing a cold solution of coupling components (0.003 mol, 0.45 g) is mixed with the diazonium salt solution. There is stirring of the reaction mixture for a further 2 h at 0 °C, maintaining the pH at 5-6 by adding sodium bicarbonate solution. The purity of the resultant azo compounds is examined using thin-layer chromatography on alumina-silica plates. The product is filtered, repeatedly rinsed with water, dried, and then ethanol-recrystallized. The synthetic procedure for azo dye synthesis illustrates in Scheme 1, and Table 1 shows physical data of synthesized azo dyes.

2.2.2. *2-hydroxy-3-[(4-phenyl-1, 3-thiazol-2-yl) diazenyl-3, 4-dihydro-1-benzopyran-2-one (A1)*

The dye A1 obtained from the reaction between 2-amine-4-phenylthiazole (2 mmol) and 4-hydroxyl coumarine (2 mmol) as a reddish- colored solid had a 72 % yield, at m.p. 215-229 °C. The experimental spectra were captured on an FT-IR (KBr) υ_{max} 2973(Ar-CH), 1592(C=N), 3468(NH), 1447(N=N), 745(C-S), 3663(OH); ^{1}H- NMR - 12.5(S,1H, OH) 8.34-817(m. Ar-H), coumarin 7.84(t, Ar -H), 7.74-7.62(m, Ar-H), 7.38-7,33(m, Ar-H); ^{13}C NMR- ppm 106.92, 115.77,123.16, 132.65, 158.48,165.60. Analytical calculation for $C_{18}H_{11}N_3O_3S$: C (61.86 %) H (3.15 %) N (12.05 %) O (13.72 %) S (9.16 %). Found: C 61.79; H 3.12; N 12.01; O 13.65; S 9.15; MS m/z =350.2 [M^{+1}].

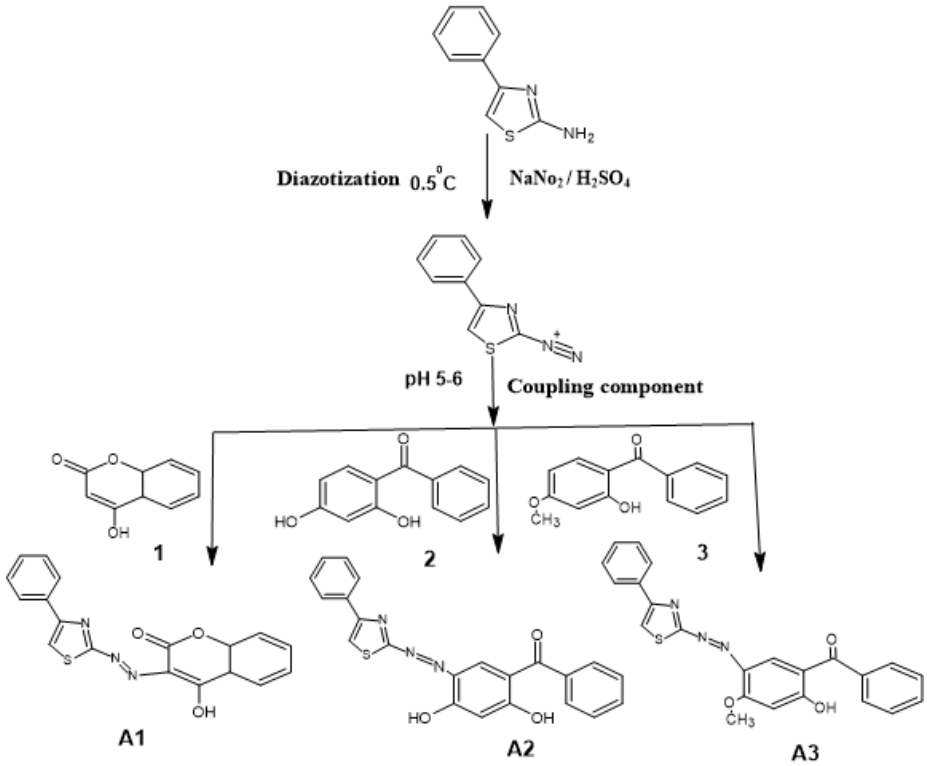

Scheme 1. Preparation of 2-amino-4-phenylethiaole azo dye (A1-A3).

2.2.3. *2, 4-dihydroxy-5-[(4-phenyl-1,3-thiazol-2yl)diazenyl]phenyl(phenyl)methanone (A2)*

The dye A2 was obtained from the reaction between 2-amine-4-phenylthiazol (2 mmol) and 2.4 dihydroxybenzophenone (2 mmol) as a reddish-yellow colored solid with a yield of 54%. m.p. 185-188 °C. The experimental spectra were captured on an FT-IR (KBr) υ_{max} 298(Ar-CH), 1594(C=N), 3555(NH), 1488(N=N), 781(C-S), 3663(-OH); ^{1}H-NMR- 6.41 (S, 1H) thioazole proton), 7.18–7.53(m. Ar-H) 8.34(m, Ar-H) 10.81(S.OH) 12.21(S, OH); ^{13}C NMR-ppm 102.73, 112.42, 123.66, 137.97, 164.90, 198.67. Analytical calculations for $C_{22}H_{15}N_3O_3S$ (65.82 %) H (3.77 %) N (10.47 %) O (11.95 %) S(7.99 %). Found: C 65.62; H 3.54; N 10.34; O 11.84; S 7.86; MS m/z =402.6 [M^{+1}].

2.2.4. *2-hydroxy-4-methoxy-5-[-(4-phenyl-1,3-thiazol-2-yl)diazenyl]phenyl(phenyl) methanone (A3)*

The dye A3 obtained from the reaction between 2-amine-4-phenylthiazole (2 mmol) and 2-hydroxy-4-methoxybenzophenone (2 mmol) as a reddish-orange colored solid with a yield of 60 %. m.p. 221-225 °C, FT-IR (KBr) υ_{max}. 2982(Ar-CH), 1517(C=N), 2470(NH), 1442(N=N), 735(C-S), 3681(OH). ^{1}H-NMR - 3.84(S.OCH_3), 6.59(S. Ar-H), 7,42-7.65(m,

Ar-H), 12.09(S.OH); ^{13}C NMR - ppm, 40.12, 106.99, 117.84, 121.23, 137.81, 165.37, 198.65. $C_{23}H_{17}N_3O_3S$. C (66.47 %) H (4.13 %) N (10.12 %) O (11.55 %) S(7.72 %). Found: C 66.30; H 4.10; O 10.09; S 6.68; MS m/z = 414.9 [M^{+1}].

Table 1. Physical data of synthesized azo dyes.

Dyes	Mol. Formula	M.P. (°C)	Yield (%)	Color	Solubility
A1	$C_{18}H_{11}N_3O_3S$	225-229	72	Red	DMSO/ Acetone/Ethanol
A2	$C_{22}H_{15}N_3O_3$	185-188	54	Reddish yellow	DMSO/ Acetone/Ethanol
A3	$C_{23}H_{17}N_3O_3S$	221-225	60	Reddish orange	DMSO/ Acetone/Ethanol

2.3. *Electrochemical studies*

All the synthetic azo compounds were dissolved in DMSO for the cyclic voltammetric investigation, and 0.1 M concentrations of sulfuric acid were employed as the supporting electrolyte. The experiment was conducted in a standard three-electrode cell. For the electrochemical measurements, the working electrode was glassy carbon electrode. The electrode system known for their wide potential range and low background current, it is suitable for studying the redox behavior of organic compounds, including azo dyes. Platinum wire acts as the counter electrode, providing a path for the current and balancing the charge during the electrochemical reaction. The reference electrode is a saturated calomel electrode provide by the steady reference potential against which the working electrode potential.

The stock solution prepared by dissolves 2 mg of all azo dyes in 20 mL of DMSO, and more dilution for electrochemical quantity was tested sample preparation from the stock solution, take 1 ml of the stock solution then dilute with supporting electrolyte 9 ml of 0.1 M sulfuric acid. This provides the necessary acidic environment for the electrochemical study while also achieving a suitable concentration for measurement. This technique can be employed to examine the redox behavior of the synthesized compound. The sweep rate, potential range, and other parameters should be optimized based on the specific characteristics of the dyes being studied.

3. Results and Discussion

3.1. *Infrared spectra*

Table 2 shows the absorption frequencies of significant functional groups in FT-IR spectral data of synthesized azo dyes (A1-A3)**.** All of the prepared azo dyes displayed significant infrared bands. The OH group is responsible for a broad absorption band in the 3663–3681 cm^{-1} range. Other values at 2973-2982 cm^{-1} (C-H aromatic) 1658-1696 cm^{-1} and (C=O) 1517-1592 cm^{-1} due to azo group is 1412-1447 cm^{-1} and 735-789 cm^{-1} C-S stretching vibrations. The figure is shown in supplementary figure file S1–S3.

Table 2. FT-IR spectral data of synthesized azo dyes (A1-A3).

Compound	(OH)	(CH)	(C=O)	(C=N)	(N=N)	(C-S)
A1	3663	2973	1696	1592	1447	745
A2	3663	2981	1658	1594	1488	789
A3	3681	2982	1666	1517	1442	735

3.2. *Electronic absorption spectra*

Electronic absorption spectra of the synthesized azo compound be analyzed at room temperature in three solvents: DMSO, Ethanol, and acetone at a concentration 3×10^{-5} mol L^{-1}. The azo group and the electrons of the aromatic system cause the first band, which corresponds to the n→π* transition, to emerge in the 200–400 nm region [29]. The second band is attributed to the n→ π* and appears in the 350–580 nm range shown in Table 3, and the figure shown in supplementary file S4-S6. The n→π* transition in azo compounds, particularly those containing an azo (-N=N-) group, is an important aspect of their electronic properties. The nitrogen atoms in the azo group each have a lone pair of electrons that can participate in interactions with solvent molecules, when the solvent is more polar, it can stabilize the electron density around the nitrogen, enhancing the overall electron delocalization within the dye's structure. This leads to a bathochromic shift, as the electronic transitions become more favourable at longer wavelengths [30].

Table 3. Absorption spectral data for the synthesized azo dyes.

Compound	λ_{max} nm			log ε		
	DMSO	Ethanol	Acetone	DMSO	Ethanol	Acetone
A1	413	389	386	495	501	480
A2	411	388	381	497	495	477
A3	391	382	383	502	493	472

3.3. *^{1}H NMR*

The synthesized azo dyes ^{1}H NMR spectra, as shown in Figs. S7-S9. The compound A1 represents aromatic protons that can be found between 7.002 and 8.343 ppm, while the methoxy protons resonate at 4.314 ppm. The OH group protons resonate at 12.569 ppm. The methoxy proton in the A2 molecule resonates at 3.710 ppm, while all aromatic protons resonate among 6.414- 8.341 ppm. The OH is resonating between 10.850 and 12.23 ppm. The A3 molecule exhibited signals at aromatic proton 6.523-7.665 ppm and methoxy 3.441-3.848 ppm. 12.092 ppm is the OH group proton.

3.4. *^{13}C NMR*

The azo dyes ^{13}C NMR spectra were recorded in DMSO–d_6. In the spectrum of the A1 compound 38.872- 40.128 ppm of an aliphatic carbon atom, signals at 116.32 ppm with the carbon atom is the coupling element. There was a resonance between 116.77-153.48 ppm for the aromatic carbonyl thiazole ring and 161.87-165.60 ppm for the carbonyl (carbon).

The A2 compound carbonyl carbon (C=O) and (C-OH) had respective of 164.94 and 198.64 ppm, the coupling component's carbon atom connected to the azo group is 102.73–108.21 ppm, whereas the aromatic carbon thiazole ring has a concentration of 123.66–137.97 ppm. The range of 38.882- 40.118 ppm was where the aliphatic carbon atom displayed signals. The A3 compound carbonyl carbon displayed signals in the region (C=O) 163.85 ppm and (C-OH) 198.65 ppm in the spectrum. In the thiazole ring, the aromatic carbon formed signals that resonate in the 121.23–137.81 ppm range. The region 113.84–117.81 ppm was found for the carbon molecule of the coupling components connected to the azo group, while the methyl carbon displayed signals in the 38.87- 40.12 ppm range as shown in Figs. S10- S12.

3.5. *Mass spectra*

The mass spectra of azo dyes peak at 350.2 m/z, 402.6 m/z, and 414.9 m/z for Compounds A1, A2, and A3, respectively, matching their [m+1] ion peaks, which are in good accord with the proposed molecular formula. These peaks support the suggested formula to verify that their molecular weight and formula weight are equivalent as shown in Figs. S13-S15.

3.6. *Electrochemical studies*

3.6.1. *Irreversible electrochemical character of azo dye at glassy carbon electrode (GCE)*

The electrochemical experiment involving the synthesized azo compounds (A1, A2, and A3) were conducted using cyclic voltammetry (CV) in a solvent (DMSO) with a supporting electrolyte of 0.1 M H_2SO_4 (Fig. 1). The study focused on the reduction behavior of the azo dyes, particularly the impact of scan rates and concentration. Below is a detailed interpretation of the observed voltammograms and the reduction processes. Two distinct reduction peaks were observed for each compound, indicating two-step reduction process. The peaks correspond to the breaking of the azo linkage (N=N). Irreversibility is the absence of anodic peaks in the cyclic voltammograms confirms that the reduction process is irreversible [31]. This irreversibility is attributed to the stability of the reduced products (hydrazo and amine compounds). The reduction of azo compounds typically involves $2e^-/H^+$ or $4e^-/H^+$ processes, depending on the substituents and experimental conditions $2e^-/H^+$ reduction is produces hydrazo intermediates. $4e^-/H^+$ reduction yields amino compounds as final products, especially in the presence of strong electron-donating groups.

Interpretation of Peaks are first reduction peak associated with the initial reduction of the azo group (N=N) to a hydrazine-like intermediate the reaction involves the transfer of 2 electrons and 2 protons ($2e^-/H^+$). Second Reduction Peak corresponds to the further reduction of the hydrazine intermediate to amine products the reaction involves an additional 2 electrons and 2 protons (total of $4e^-/H^+$) [32]. The reduction peak potentials for the compounds A1: first peak is -0.401 V, second peak is 0.781 V, Compound A2: first peak is -0.59, second peak is-1.060 V and compound A3: first peak is -0.389 V, second

peak is -0.946 V. The differences in peak potentials among the compounds (A1, A2, and A3) highlight the influence of substituents on the reduction mechanism. This study provides valuable insights into the electrochemical behavior of azo dyes and their reduction processes.

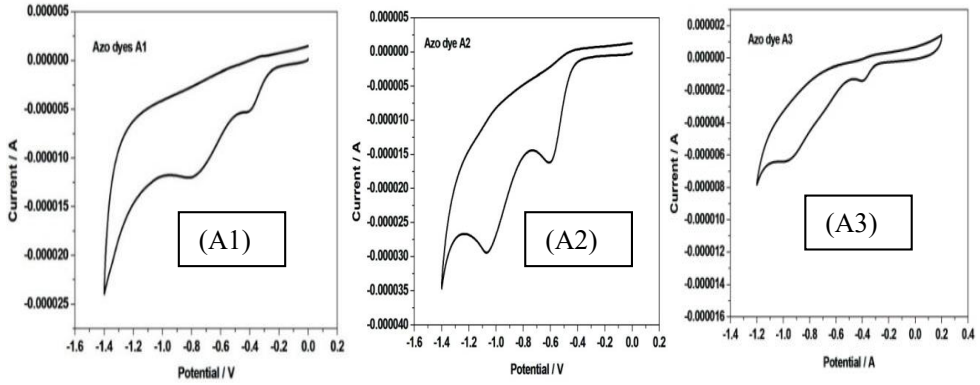

Fig. 1. Electrochemical reduction of synthesised compound (A1-A3) at GCE in 0.1 M H_2SO_4 at scan rate 100 $mV^{-1}s$.

3.6.2. *Impact of scan rate*

The impact of scan rate on the electrochemical reduction of the azo dyes (A1, A2, and A3) at a glassy carbon electrode (GCE) in 0.1 M H_2SO_4 as the supporting electrolyte was investigated. The results are summarized in Fig. 2 as the scan rate increases from 50 to 250 mV/s, the peak current (Ip) for the azo dyes increases significantly. This is because faster scan rates reduce the time available for the reactants (azo compounds) to diffuse to the electrode surface, but they also enhance the charge transfer kinetics, leading to higher peak currents [33]. The Fig. 3 shows the linear relationship between log Ip and log ν (scan rate) suggests that the electrochemical process is diffusion-controlled. In a diffusion-controlled process, the peak current is directly proportional to the concentration of the reactant at the electrode surface, which is influenced by the rate of diffusion and Fig. 4 shows the linear correlation between Ip and $\nu^{1/2}$ is the linear relationship between the square root of the scan rate ($\nu^{1/2}$) and the peak current (Ipc) further confirms that the process is diffusion-controlled [34]. This is a common characteristic of electrochemical reactions where the rate of reaction is limited by the diffusion of reactants to the electrode surface. The linear correlations for the compounds are A1 compound is linear correlation is log Ip = 0.13718 log υ + 1.19354, R^2 = 0.99854. A2 compound is log Ip = 1.4633 log υ + 0.0947, R^2 = 0.99915 and A3 compound are log Ip = 1.066 log υ+2.751, R^2 = 0.9752 was recorded as shown in a graph and the other hand study involving cyclic voltammetry, linear correlation between the square root of ($\nu^{1/2}$) of the scan rate and the peak current (Ipc). This correlation typically indicates that the Ipa = 0.0949+1.5348ν1/2, r^2 = 0.9903. Ipa = 0.0940+1.4635348$\nu^{1/2}$, r^2 = 0.999 and Ipa = 0.2255+4.2106 $\nu^{1/2}$, r^2 = 0.9919 and electrochemical process is diffusion-

controlled [35]. The linear relationships between log Ip vs. log ν and Ipc vs. $\nu^{1/2}$ confirm that the electrochemical reduction of the azo dyes is diffusion-controlled [35]. This means that the rate of the electrochemical reaction is limited by the diffusion of the azo compounds to the electrode surface.

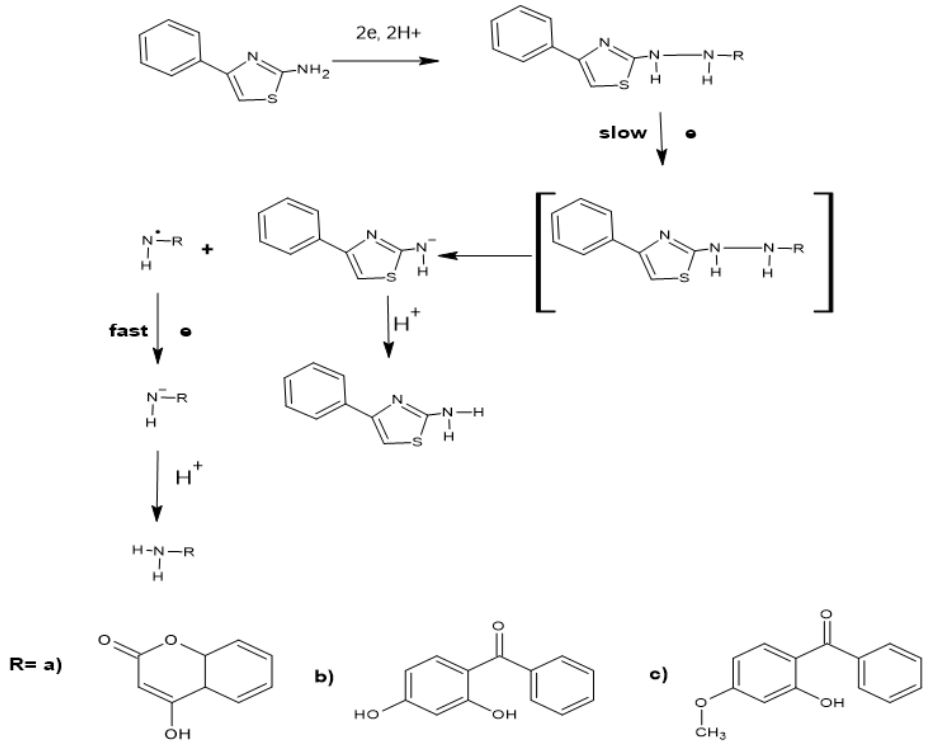

Scheme 2: Reduction mechanism of azo molecules (A1-A3)

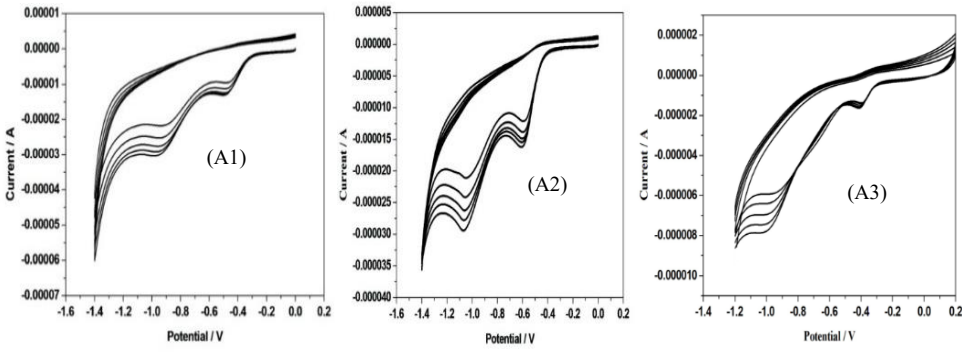

Fig. 2. Graph of current v/s different scan rate (50 to 250 mVs^{-1}) for compounds (A1-A3).

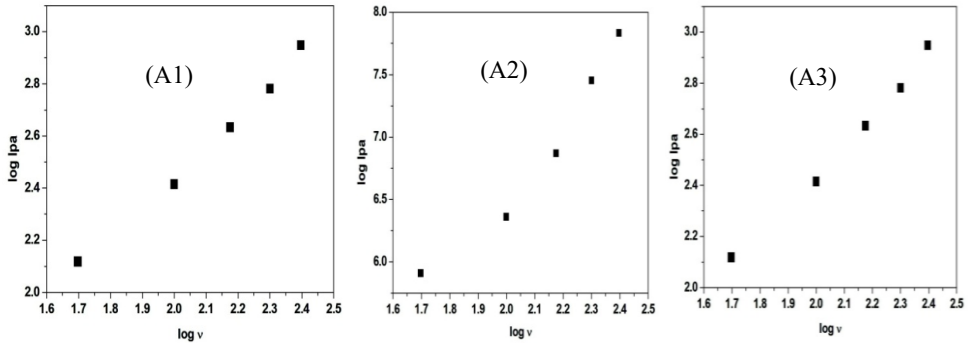

Fig. 3. Log of current v/s log of scan rate (50 to 250 $mV^{-1}s$) for compounds (A1-A3).

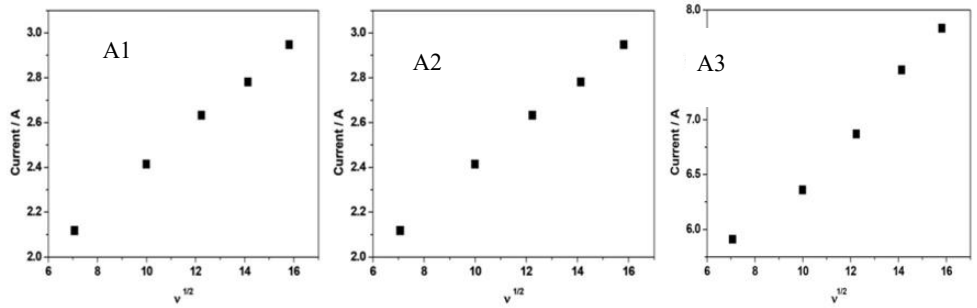

Fig. 4. Current v/s square root of scan rate (50 to 250 $mV^{-1}s$) for compounds (A1-A3).

3.6.3. *Impact of concentration*

The reduction peak currents for different concentrations of the compounds A1, A2, and A3 voltammograms are shown in Fig. 5. As the concentrations of these compounds increase from 10 µM to 50 µM for (A1-A3), there is a corresponding rise in the reduction peak current. This indicates that higher concentrations lead to greater reduction [36]. The correlation coefficient values are $r^2 = 0.9899$, 0.9987, and 0.9954. The LOD and LOQ were proposed by using the equation (1) and (2).

$$LOD = 3S/M \quad \text{----------} \quad (1)$$

$$LOQ = 10S/M \quad \text{----------} \quad (2)$$

Where M is the slop the calibration plots and S is the standard deviation, LOD, and LOQ were discovered to be compound (A1-A3) were found to be 0.1819 µM, 0.1276 µM, 0.4004 µM and 0.273 µM, 0.192 µM, 1.334 µM respectively.

The LOD values indicate the lowest concentration of the azo dyes that can be reliably detected, while the LOQ values indicate the lowest concentration that can be quantified with acceptable accuracy. The low LOD and LOQ values for A1 and A2 suggest that these compounds can be detected and quantified at very low concentrations, making them suitable for sensitive analytical applications. The slightly higher LOD and LOQ values for A3 indicate that it is less sensitive compared to A1 and A2, which may be due to differences in

the electrochemical behavior or molecular structure of the compound. The results provide valuable insights into the electrochemical behavior of azo dyes and their potential applications in electrochemistry**.**

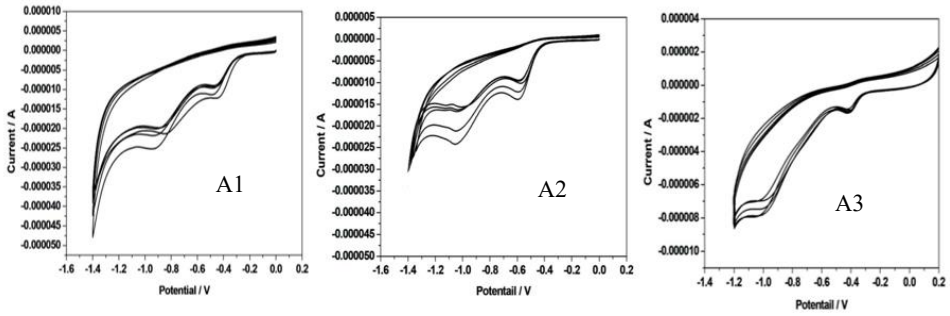

Fig. 5. Cyclic voltammograms of synthesized compounds (A1-A3).

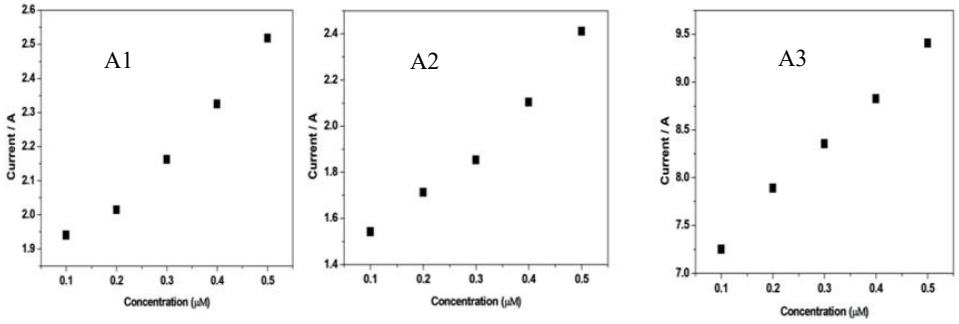

Fig. 6. Current at different concentrations of synthesized compounds (A1-A3)

4. Conclusion

Three new azo dyes were synthesized from 2-amino-4-phenylthiazole using a well-known diazotization process. Different analytical techniques were used for the characterization of azo dyes such as FT-IR, UV-Vis, NMR, mass spectrometry, and elemental analysis. UV-Vis allows a comprehensive understanding of the molecular structure, solvent interactions, and substituent effects on azo dyes. The solvent's ability to interact with the nitrogen atoms of the azo group can stabilize electron density, affecting the dye's electronic properties. Additionally, the presence of electron-withdrawing substituents or electron-donating on the aromatic rings influences the dye's absorption spectrum, causing bathochromic shifts and thereby affecting the dye's color and functionality. Moreover, cyclic voltammetric analysis was used to examine the electrochemical behavior of the azo compound at GCE. The studies showed that the reduction of all azo compounds continues to the hydrazo stage, breaking -NH-NH- bonds into their resultant amines as end products. This shows that, in an acidic environment, the reduction of an azo group involves four electrons and four protons is irreversibly. Furthermore, when the concentration of solution increases, the reduction wave

potentials decrease and the electrochemical process is diffusion controlled, because the synthetic dye has chromophore in its structures, it exhibits good coloring qualities and functions well as an electron exchange mediator during the redox process.

References

1. M. R. Yazdanbakhsh, A. Mohammadi, and M. Abbasnia, Spectrochim. Acta A. Mol. Biomol. Spectrosc. **77**, 1084 (2010). https://doi.org/10.1016/j.saa.2010.08.079
2. B. Derkowska-Zielinska, L. Skowronski, A. Biitseva, A. Grabowski, M. K. Naparty, V. Smokal, and O. Krupka, Appl. Surface Sci. **421**, 361 (2017). https://doi.org/10.1016/j.apsusc.2016.12.080
3. A. S. Shekhawat, N. P. Singh, and N. S. Chundawat, J. Sci. Res. **14**, 387 (2022). http://dx.doi.org/10.3329/jsr.v14i1.54814
4. Z. Ghasemi, S. Azizi, R. Salehi, and H. S. Kafil, Monatsh. Chem. **149**, 149 (2018). https://doi.org/10.1007/s00706-017-2073-y
5. S. Benkhaya, S. M'rabet, and A. El Harfi, Heliyon **6**, 3271 (2020). https://doi.org/10.1016/j.heliyon.2020.e03271
6. M. Henary and A. Levitz, Dye Pig. **99**, 1107 (2013). https://doi.org/10.1016/j.dyepig.2013.08.001
7. M. M. Aftan, M. A. Toma, A. H. Dalaf, E. Q. Abdullah, and H. K. Salih. Egypt. J. Chem. **64**, 2903 (2021). https://dx.doi.org/10.21608/ejchem.2021.55296.3163
8. K. S. D. Djeukoua, E. S. Fondjo, J. D. Tamokou, J. Tsemeugne, P. F. W. Simon, A. Tsopmo, F. M. M. Tchieno, S. E. Ekom, C, N. Pecheu, I. K. Tonle, and J. R. Kuiateb, Org. Chem. 416 (2019). https://doi.org/10.24820/ark.5550190.p010.994
9. H. S. H. Mohamed, M. N. M. Gad, and S. A. Ahmed, Int. J. Adv. Res. **5**, 2426 (2017). https://dx.doi.org/10.21474/IJAR01/4990
10. N. N. Ayare, S. H. Ramugade, and N. Sekar, Dye. Pig. **163**, 692 (2019). https://doi.org/10.1016/j.dyepig.2018.12.050
11. M. M. M Raposo, M. C. R. Castro, M. Belsley, and A. M. C. Fonseca, Dyes Pigments **91**, 454 (2011). https://doi.org/10.1016/j.dyepig.2011.05.007
12. P. Kumari and M. Singh, J. Sci. Res. **17**, 341 (2025). https://doi.org/10.3329/jsr.v17i1.74922
13. M. M. Aftan, M. A. Toma, A. H. Dalaf, E. Q. Abdullah, and H. K. Salih, Egypt. J. Chem. **64**, 2903 (2021). https://dx.doi.org/10.21608/ejchem.2021.55296.3163
14. M. R. Maliyappa, J. Keshavayya, M. S. Sudhanva, and I. Pushpavathi, J. Mol. Struc. **1247**, ID 131321 (2022). https://doi.org/10.1016/j.molstruc.2021.131321
15. R. Podsiadły, J. Sokołowska, A. Marcinek, J. Zielonka, A. Socha, and Kaźmierska, M. J. Photochem. Photobiol. A Chem. **171**, 69 (2005). https://doi.org/10.1016/j.jphotochem.2004.09.009
16. P. R. Sonune, U. P. Manik, and P. L. Mishra, J. Sci. Res. **17**, 21 (2025). https://doi.org/10.3329/jsr.v17i1.72075
17. M. Ghalkhani, J. Beheshtian, and M. Salehi, Mat. Sci. Eng. C **69**, 1345 (2016). https://doi.org/10.1016/j.msec.2016.08.031
18. H. C. Hsu, C. H. Wang, Y. C. Chang, J. H. Hu, B. Y. Yao, and C. Y. Lin, J. Phys. Chem. Solids **85**, 62 (2015). https://doi.org/10.1016/j.jpcs.2015.04.010
19. R. S. Vishwanath and S. Kandaiah, J. Mat. Chem. A **5**, 2052 (2017).
20. A. A. Adeniyi, T. L. Ngake, and J. Conradie, Electroanalysis **32**, 2659 (2020). https://doi.org/10.1002/elan.202060163
21. S. J. Almehmadi, A. Alharbi, M. M Abualnaja, K. Alkhamis, M. Alhasani, S. H. Abdel-Hafez, and N. M. El-Metwaly, Arab. J. Chem. **15**, ID 103586 (2022). https://doi.org/10.1016/j.arabjc.2021.103586
22. G. Anand, M. Sivasubramanian, I. Manimehan, P. Jagdish, P. Paramasivam, and R. K. Asmitha, J. Sci. Res. **17**, 151(2025). https://doi.org/10.3329/jsr.v17i1.74446

23. N. Uludag, G. Serdaroğlu, P. Sugumar, P. Rajkumar, N. Colak, and E. Ercag, J. Mol. Struc. **1257**, ID 132607 (2022). https://doi.org/10.1016/j.molstruc.2022.132607
24. S.C. Gavandi, S. S. Mahajan, and D. S. Sutrave, J. Sci. Res. **17**, 247 (2025). https://doi.org/10.3329/jsr.v17i1.72486
25. S. I. Kaya, S. Kurbanoglu, and S. A, Oskar, Crit. Rev. Anal. Chem, **49**, 101 (2019). https://doi.org/10.1080/10408347.2018.1489217
26. S. Harisha, J. Keshavayya, S. M Prasanna, and H. J. Hoskeri, J. Mol. Struc. **1218**, ID 128477 (2020). https://doi.org/10.1016/j.molstruc.2020.128477
27. C. T. K. Kumar, J. Keshavayya, T. Rajesh, S. K. Peethambar, and A. R. S. Ali, Org. Chem. Int. **5**, 296 (2013).
28. C. T. K. Kumar, J. Keshavayya, T. Rajesh, S. K. Peethambar, and A. R. S. Ali, Org. Chem. Int. **2013**, ID 370626 (2013). https://doi.org/10.1155/2013/370626
29. S. Antonysakthi, M. S. Selvakumar, and P. L. Prabha, J. Sci. Res. **14**, 583 (2022). http://dx.doi.org/10.3329/jsr.v14i2.54735
30. R. Podsiadły, J. Sokołowska, A. Marcinek, J. Zielonka, A. Socha, and M. Kaźmierska, J. Photochem. Photobiol. A: Chem. **171**, 69 (2005). https://doi.org/10.1016/j.jphotochem.2004.09.009
31. K. Pliuta, A. Chebotarev, A. Pliuta, and D. Snigur, Electroanalysis 33, 987 (2021). https://doi.org/10.1002/elan.202060367
32. N. M. Mallikarjuna and J. Keshavayya. J. King Saud Univ. Sci. **32**, 251 (2020). https://doi.org/10.1016/j.jksus.2018.04.033
33. B. N. Ravi, J. Keshavayya, N. Mallikarjuna, and H. M Santhosh, Chem. Data Coll. **25**, ID 100334 (2020) https://doi.org/10.1016/j.cdc.2019.100334
34. M. R. Maliyappa, J. Keshavayya, M. Mahanthappa, Y. Shivaraj and K. V. Basavarajappa, J. Mol. Struc. **1199**, ID 126959 (2020). https://doi.org/10.1016/j.molstruc.2019.126959
35. S. Harisha, J. Keshavayya, B. K. Swamy, and C. C. Viswanath, Dye Pig. **136**, 742 (2017). https://doi.org/10.1016/j.dyepig.2016.09.004
36. R. B. N. J. Keshavayya, N. M. Mallikarjuna, V. Kumar, and F. N. Zahara, Chem. Data Coll. **33**, ID 100686 (2021). https://doi.org/10.1016/j.cdc.2021.100686

Supplementary Information

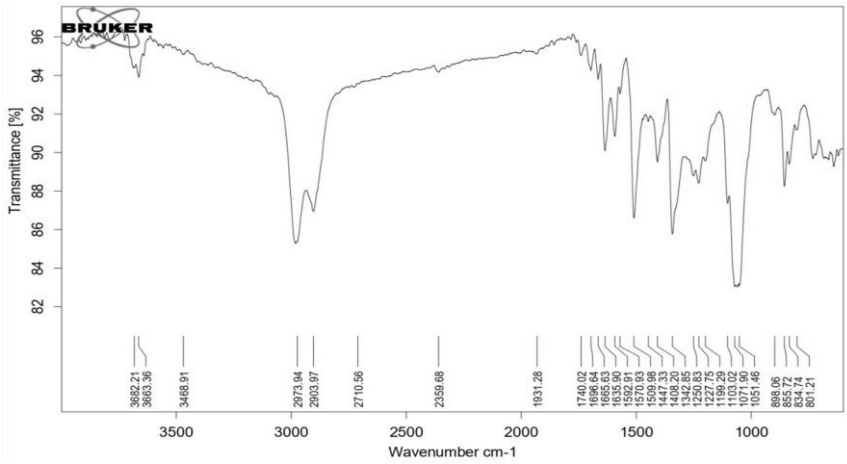

Fig. S1. FT-IR spectrum of compound A1.

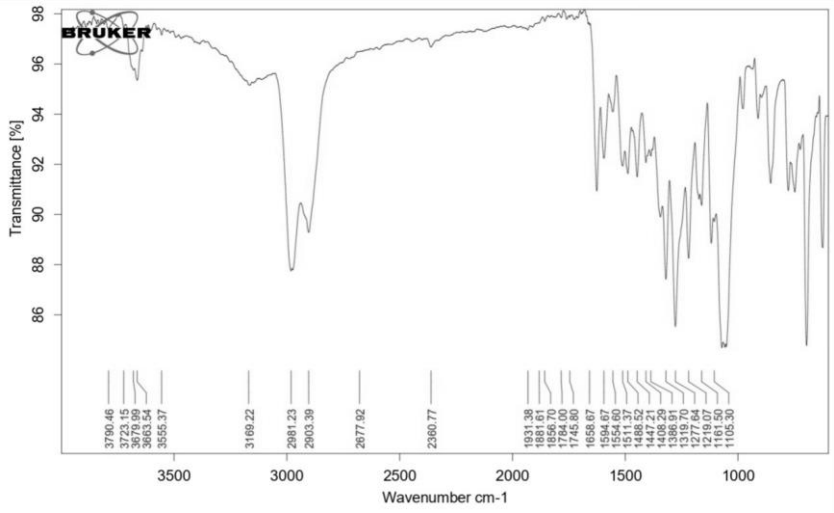

Fig. S2. FT-IR spectrum of compound A2.

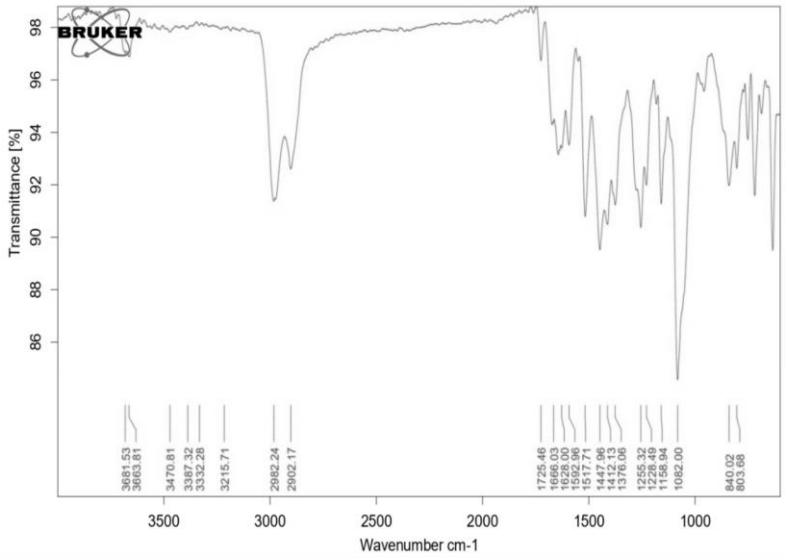

Fig. S3. FT-IR spectrum of compound A3.

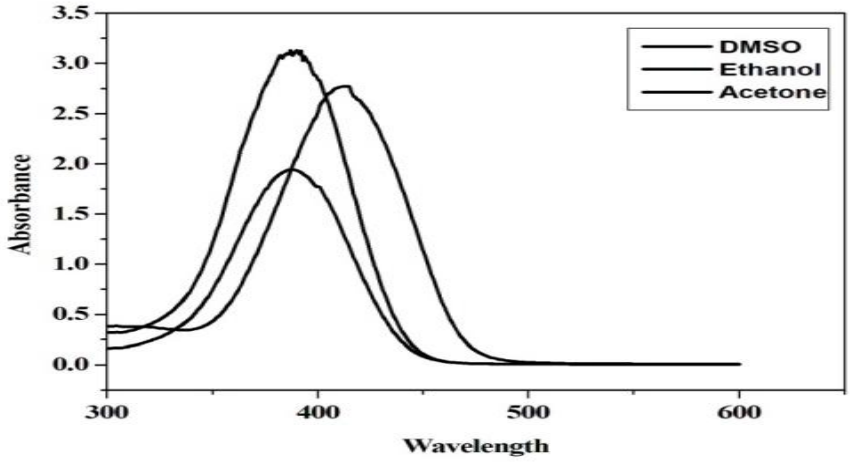

Fig. S4. UV-Visible spectrum of compound A1.

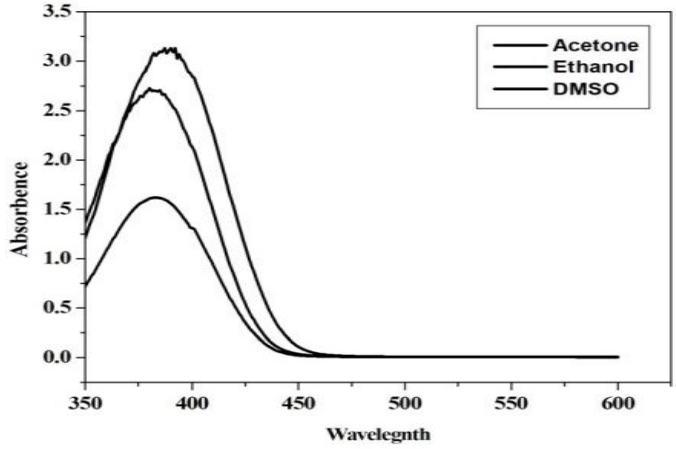

Fig. S5. UV-Visible spectrum of compound A2.

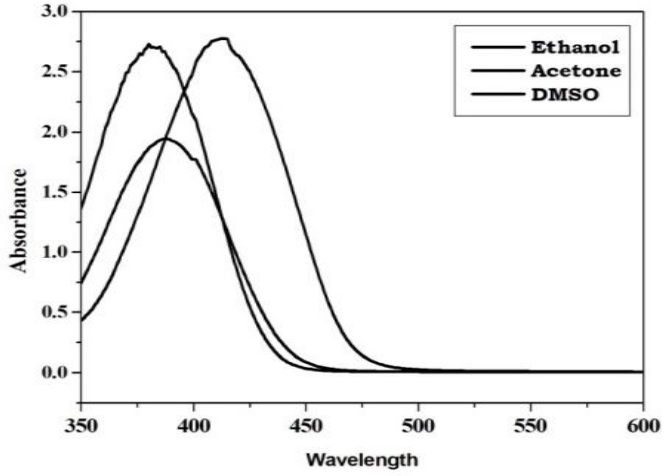

Fig. S6. UV-Visible spectrum of compound A3.

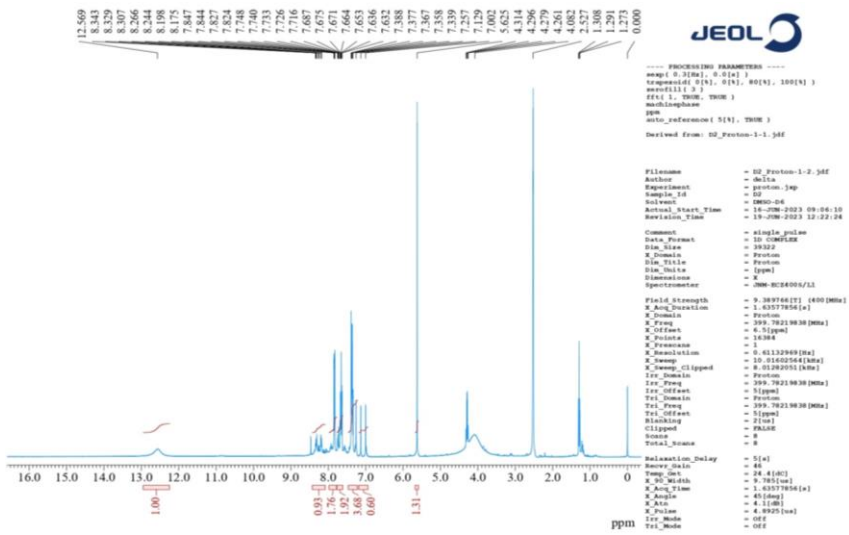

Fig. S7. [1]H NMR spectrum of compound A1.

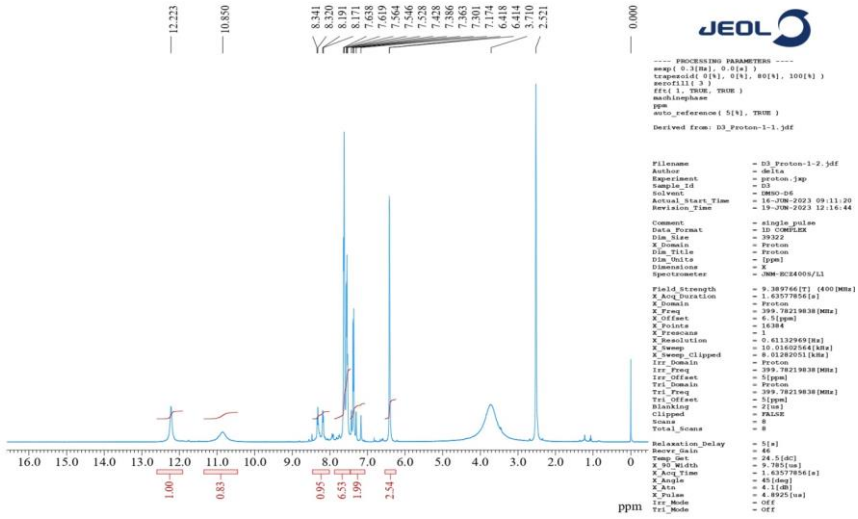

Fig. S8. [1]H NMR spectrum of compound A2.

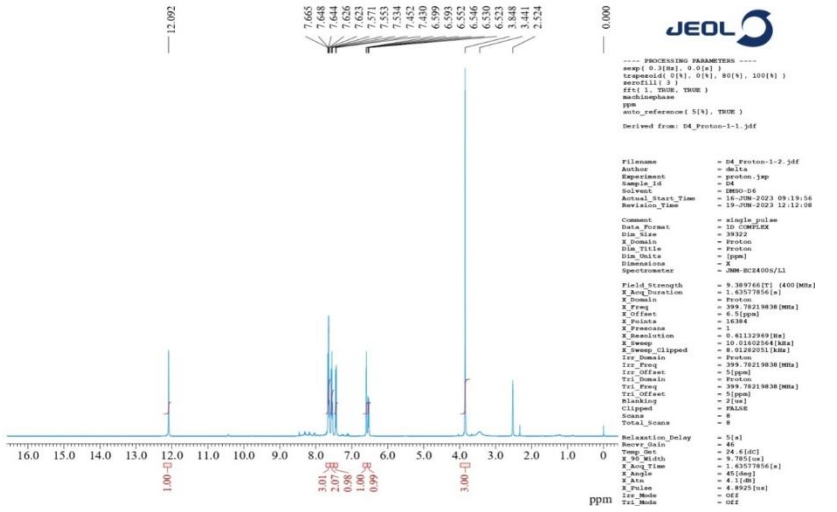

Fig. S9. [1]H NMR spectrum of compound A3.

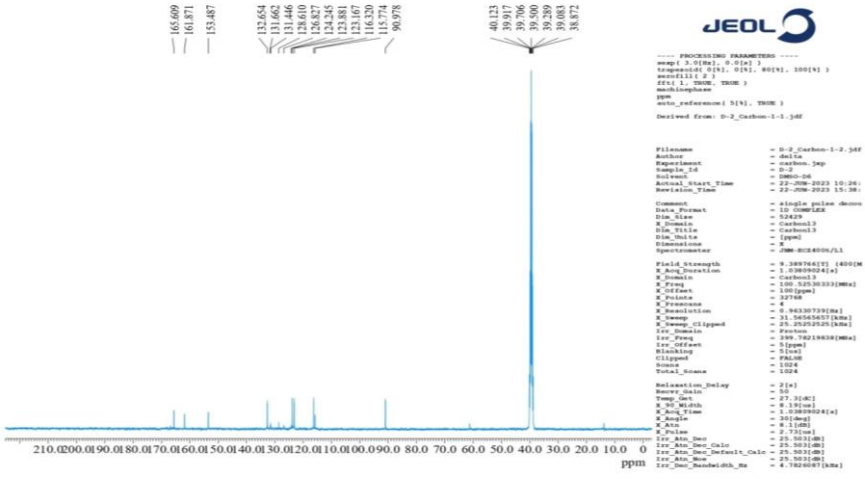

Fig. S10. [13] C NMR spectrum of compound A1.

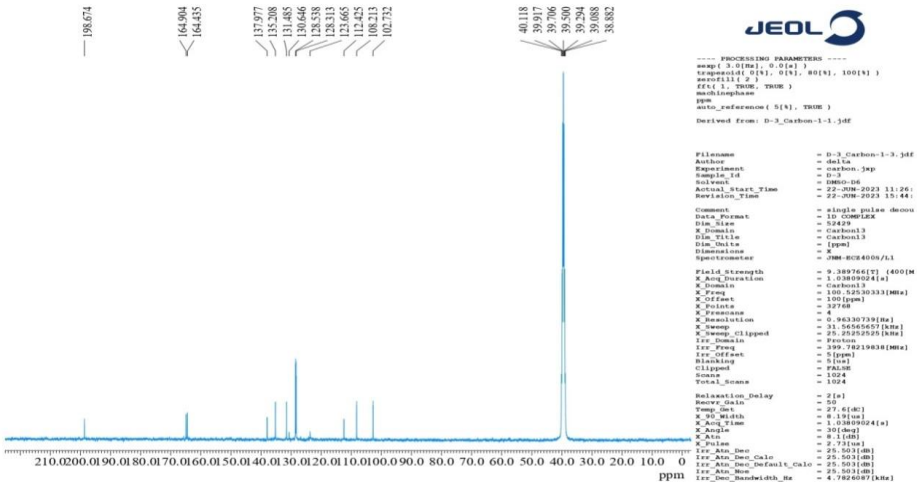

Fig. S11. [13] C NMR spectrum of compound A2.

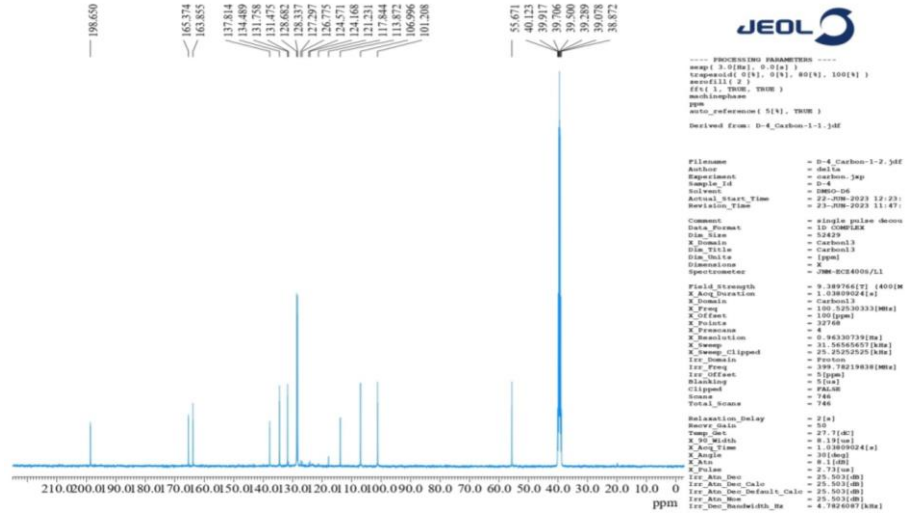

Fig. S12. [13] C NMR spectrum of compound A3.

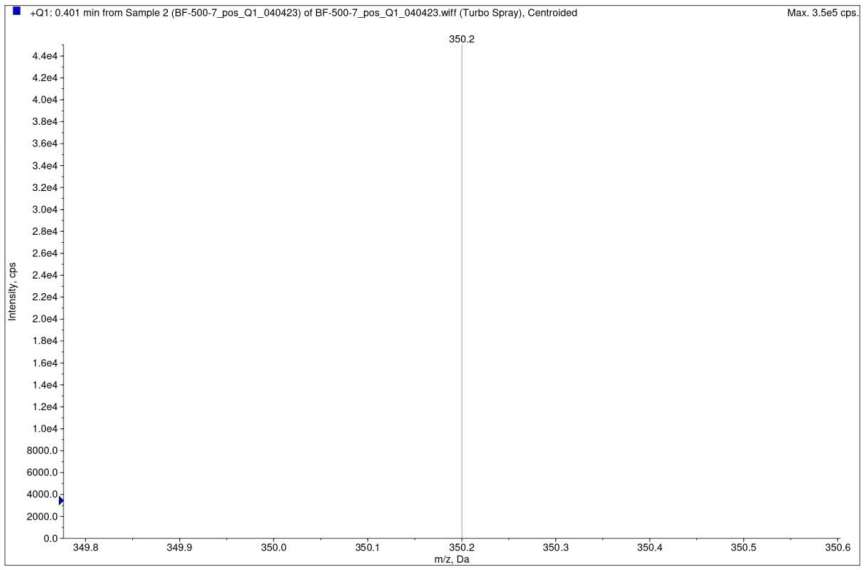

Fig. S13. Mass spectrum of compound A1.

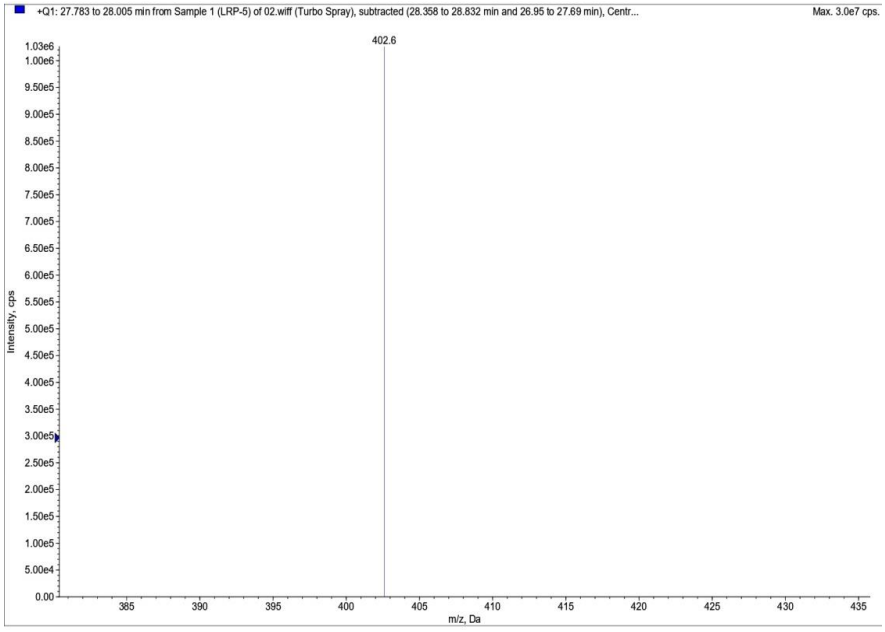

Fig. S14. Mass spectrum of compound A2.

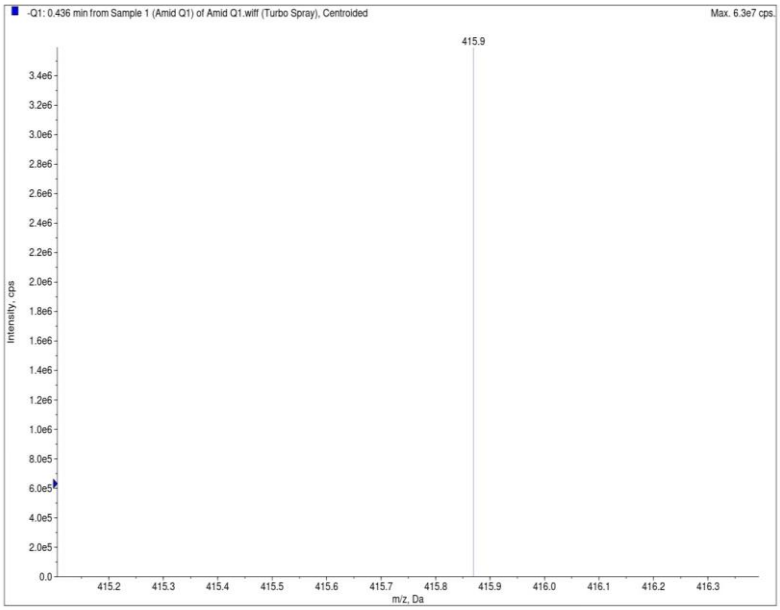

Fig. S15. Mass spectrum of compound A3.